Reprinted from The Journal of Physical Chemistry, 1991, 95.

Time-Resolved Studies of Phenol Proton Transfer in Clusters. 3. Solvent Structure and Ion-Pair Formation

Jhobe Steadman[†] and Jack A. Syage*

Aerophysics Laboratory, The Aerospace Corporation, P.O. Box 92957/M5-754, Los Angeles, California 90009
(Received: March 15, 1991)

Time-resolved resonance–ionization spectroscopy was used to measure properties of proton transfer in clusters. Ground electronic ion-pair states of phenol, stabilized in $(NH_3)_n$ and $[(CH_3)_3N]_n$ solvent clusters, were detected by their long-lived absorptions at 355 nm (>1 ns). The ionization signals $PhOH^+(NH_3)_n$ and $H^+(NH_3)_n$ exhibit a strong enhancement at $n = 4$ and 5, corresponding to a stable, closed solvent coordination shell. The detection of negative ions from ion-pair photodissociation showed no evidence of solvent-separated ion pairs. Instead, only dissociative ionization of a contact ion pair was observed. The rate of excited-state proton transfer of phenol dimer in $(NH_3)_n$ solvent clusters was measured. The phenol molecules in the dimer are inequivalent, only one of which undergoes facile proton transfer to the solvent ($1/k \simeq 50$ ps versus ≥ 500 ps for $n = 6$). Finally, solvent bonding structures were deduced from resonance–ionization mass spectra of PhOH in mixed solvent clusters $(NH_3)_m B_n$ [B = CH_3OH or $(CH_3)_3N$].

1. Introduction

Molecular clusters are small aggregates of molecules, isolated from one another, that exhibit properties intermediate between the gas phase and condensed phase.[1-3] In recent work we have exploited the cluster environment using picosecond spectroscopy to study chemistry under single-molecule solvent interactions.[4-8] The majority of cluster research depends on supersonic expansion for providing the molecular cooling and low-energy collisions necessary for cluster formation.[9] If the internal energy of the cold clusters is low relative to the photoexcitation energy, then the excited-state clusters are nearly isoenergetic and constitute a microcanonical ensemble (i.e., an ensemble of noninteracting subsystems at constant energy). The study of reactions in clusters therefore has the additional benefit of minimizing thermal averaging.

The study of microcanonical cluster chemistry and single-molecule solvation offers a new perspective on the old subject of acid–base chemistry. New discoveries are unfolding that are helping to unravel the intricacies of solvation effects. In this special issue on proton transfer we wish to present results that probe the molecular basis of solvation. Our prototype proton-transfer system is designated as $PhOH{\cdot}B_n$, where PhOH is the acid phenol and B_n is the surrounding base solvent cluster consisting of n molecules. In previous work, we focused on excited-state proton transfer (ESPT) from the S_1 state of phenol (paper 1)[6] and dissociative proton transfer in cationic phenol (paper 2)[7] solvated in clusters.

We report on three topics that highlight the role of solvent structure on proton-transfer reactions. First, we present evidence for the direct detection of ground electronic state ion-pair structures of the form $PhO^-H^+(NH_3)_n$. Although the equilibrium constant for ground ion-pair states is low for small values of n, there is an abrupt increase at $n = 4$ which can be attributed to the stability gained by closing of the first solvation shell. The proton transfer in small clusters produces contact and not solvent-separated ion pairs based on negative-ion photodissociation experiments. Second, we present measured rates of S_1 ESPT for phenol dimers in solvent clusters. Dimerization was found to impede reaction significantly relative to the monomer. It is surmised that the dimer self-association structure prevents the solvent from acting as a proton acceptor. Third, we show that the solvent structure about phenol for mixed solvents can be deduced from the relative stabilities and the dissociation patterns of the ionized clusters.

2. Experimental Section

The picosecond molecular beam apparatus has been described before;[4-6,10] hence, we give only the briefest details. The molecular beam employs a temperature-controlled pulsed supersonic nozzle which serves as the cluster source. The free-jet expansion passes through a skimmer to form a 5-mm-diameter beam at the ionization region of a time-of-flight mass spectrometer. Phenol (Aldrich, 99+%, used as is) is contained in a sample holder in the pulsed nozzle, which is heated to about 50 °C. For pure ammonia or trimethylamine (TMA) solvation, a 2-L high-pressure cylinder was filled with a sample containing 10% gaseous solvent in helium. For the mixed NH_3/TMA solvent experiments, a mixture of both gases was prepared in He. For the NH_3/CH_3OH experiments, a pure ammonia/He sample was passed through a bubbler containing CH_3OH. Each of these solvent/He samples was flowed over the phenol contained in the pulsed valve. The flow mixture, at a typical backing pressure of 35 psi, was expanded through a nozzle with a 750-μm-diameter aperture and 60° conical throat.

The picosecond laser is based on a pulsed (10 Hz) active/passive mode-locked Nd:YAG laser, which produces output at 532 nm (25-ps pulses), 355 nm (25 ps), and 266 nm (18 ps). Time-resolved spectra were recorded by delaying a probe pulse λ_2 relative to a pump pulse λ_1 using a scanning optical delay line.[4-6] We refer to the sequence and the delay time t by the designation λ_1–t–λ_2. Calculated curves are fitted to the data using a convolution that assumes a Gaussian-shaped instrument function (typically 25–30 ps, fwhm).

3. Background

It is useful to summarize some properties concerning proton transfer in $PhOH{\cdot}B_n$ clusters. The reaction coordinate for proton transfer is composed of a curve crossing involving a short-range covalent bonding potential (e.g., S_0, S_1, and ground-state cation) and a long-range Coulombic ion-pair potential (or electrostatic hydrogen-bond potential for the ion).[6] Calculated curves from ref 6 are reproduced in Figure 1 for the states relevant to this discussion. The long-range potentials represent extended O–H configurations that dissociate to form protonated solvent H^+B_n. These curves are understandably very sensitive to solvent basicity (i.e., proton affinity). The interaction of these states with the

[†] National Research Council postdoctoral associate.

(1) Maier, J. P., Ed. *Ion and Cluster Ion Spectroscopy and Structure*; Elsevier: New York, 1989.
(2) Garvey, J. F.; Peifer, W. R.; Coolbaugh, M. T. *Acc. Chem. Res.* **1991**, *24*, 48.
(3) Märk, T. D.; Castleman, Jr., A. W. *Adv. At. Mol. Phys.* **1985**, *20*, 65.
(4) Syage, J. A.; Steadman, J. *Chem. Phys. Lett.* **1990**, *166*, 159.
(5) Steadman, J.; Syage, J. A. *J. Chem. Phys.* **1990**, *92*, 4630.
(6) Syage, J. A.; Steadman, J. *J. Chem. Phys.* **1991**, *95*, 2497.
(7) Steadman, J.; Syage, J. A. *J. Am. Chem. Soc.* **1991**, *113*, 6786.
(8) Steadman, J.; Fournier, E. W.; Syage, J. A. *Appl. Opt.* **1990**, *29*, 4962.
(9) Kappes, M.; Leutwyler, S. In *Atomic and Molecular Beam Methods*; Scoles, G., Ed.; Oxford University Press: New York, 1988; Vol. I, p 380.
(10) (a) Syage, J. A. *J. Chem. Phys.* **1990**, *92*, 1804. (b) Syage, J. A. *J. Phys. Chem.* **1989**, *93*, 107.

0022-3654/91/2095-10326$02.50/0

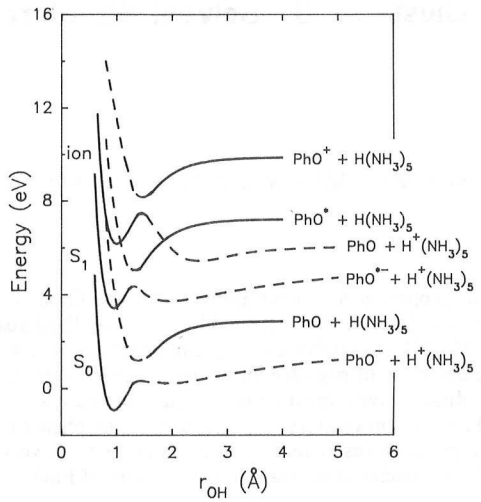

Figure 1. Potential energy curves for $PhOH\cdot(NH_3)_5$ (adapted from ref 6). Solid lines correspond to short-range covalent PhO–H bonds, and dashed lines correspond to long-range ion-pair PhO^-–H^+ or ion–dipole PhO–H^+ bonds. The latter curves dissociate to form protonated solvent $H^+(NH_3)_n$. The crossing regions define the reaction thresholds for proton transfer. The magnitude of the splitting at the crossings is not known. Zero energy corresponds to isolated phenol ground electronic state minimum.

solvent is the primary driving force to proton transfer.

Figure 1 represents the case for $B_n = (NH_3)_5$. Previous picosecond measurements indicate that proton transfer in the excited S_1 state (ESPT) is exothermic at this cluster size.[5,6] In that work, a 266-nm pulse (4.66 eV) excites the S_1 state and a delayed probe pulse samples the extent of proton transfer by ionizing the locally excited S_1 reactant and the ion-pair product states. These two forms are distinguishable because ionization of the reactant state produces a strongly bound $PhOH^+\cdot B_n$ ion, whereas ionization of the extended ion-pair state produces a weakly bound ion that dissociates to H^+B_n with high efficiency. The presence of H^+B_n in the mass spectrum is a signature for the ionization of an intermediate neutral ion-pair structure.[7]

The ion-pair minima energies decrease significantly relative to the locally excited minima for increasing cluster size. The measured critical solvent size of $n = 5$ for ESPT suggests that the reaction is slightly exothermic at this cluster size.[5,6] This would place the ion-pair minima energy at $\simeq$3.4 eV versus a calculated energy of 4.0 eV in Figure 1. The calculated potential curves (Figure 1) do not consider stabilization of the negative ion, nor is the enthalpy measured from the zero-point levels (large for the inner well and small for the outer well).[6] Including these effects would improve the agreement between experiment and calculation.

4. Ion-Pair States from Proton Transfer in Clusters

4.1. Detection of Ground Electronic Ion-Pair States. In Figure 2 we present the signal intensities of $PhOH^+(NH_3)_n$ and $H^+(NH_3)_n$ as a function of n for 355–t–266 nm excitation and delayed ionization and compare them to the ion intensities formed by either color alone (Figure 2a,b). There is clear evidence of a two-color enhancement of both ions for $n \geq 4$. The correlated two-color signal, obtained by subtracting the one-color contributions from the total signal, is represented as histograms in Figure 2c,d. Time-resolved measurements in Figure 3 establish that the 355-nm absorbing species is long-lived. A curve corresponding to infinite lifetime is drawn through the data for comparison. There is some evidence of a fast transient ($\simeq$50 ps); however, the underlying signal shows little indication of decay over the 200-ps duration of the scan. Although the signal for $t < 0$, due to 266-nm excitation to S_1 phenol and 355-nm ionization, yields a much stronger signal than for $t > 0$, the 355-nm absorbing state is not insignificant, as defined by comparing the ion signal at $t > 0$ to the single-color signal level.

The 355-nm absorbing species is assigned to the ground electronic ion-pair state of phenol on the following basis: (1) PhO^-H^+

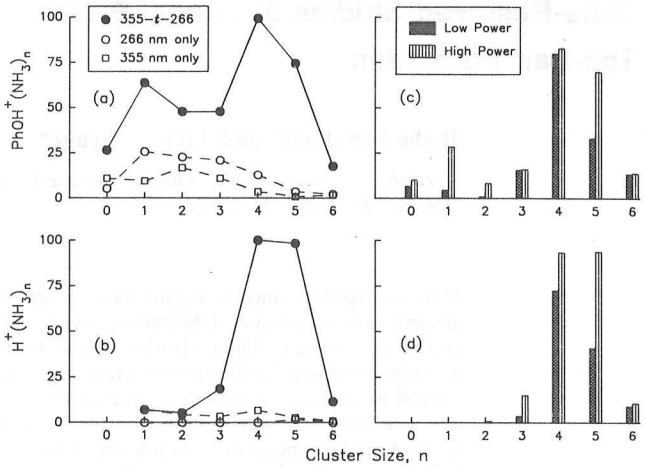

Figure 2. Relative abundance of $[PhOH]^+\cdot(NH_3)_n$ and $H^+(NH_3)_n$ following ionization of 355-nm absorbing clusters. (a,b) The total 355–t–266 nm (t = 100 ps) signal is plotted along with the single-color signals. Pulse energies were 200 μJ (355 nm) and 10 μJ (266 nm) focused to 2-mm-diameter at the molecular beam. (c,d) Correlated 355–t–266 nm signals obtained by subtracting the sum of the one-color signals from the two-color signal in (a) and (b). High-power pulse energies are listed above; low-power pulse energies are about 50% of above.

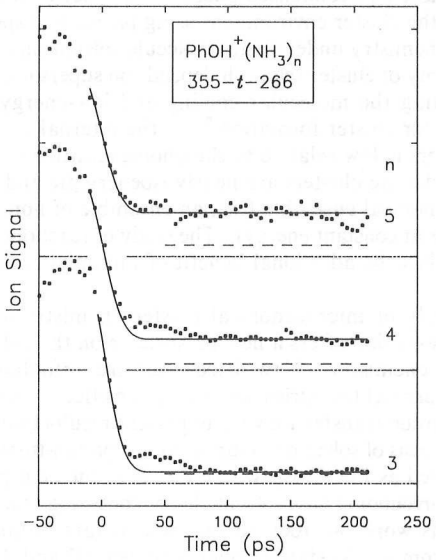

Figure 3. Time dependence for the 355-nm absorbing clusters. The calculated curves represent infinite lifetime. The (–··–) lines denote the baseline, and the (– – –) lines represent the sum of the 355- and 266-nm single-color signals.

absorbs strongly at this wavelength. The reported peak in the broad emission band of $PhO^*\text{-}H^+$ is λ_{max} = 345 nm in monoethylamine clusters and λ_{max} = 340 nm in 10^{-4} M NaOH in ethanol solution.[11] (2) Ionization leads to a large yield of $H^+(NH_3)_n$ which is regarded as a signature of an intermediate ion-pair state.[7] (3) The $S_0 \rightarrow S_1$ transitions of the covalent $PhOH\cdot(NH_3)_n$ clusters occur at too high an energy to be excited at 355 nm, even when allowing for solvent shifts [the origin transition occurs at 275.1 nm (n = 0), 280.0 nm (n = 1), 281.3 nm (n = 2), and 282.9 nm (n = 3)].[12-14] (4) The 355-nm resonance ionization signal increases significantly for tri-

(11) Jouvet, C.; Lardeux-Dedonder, C.; Richard-Viard, M.; Solgadi, D.; Tramer, A. *J. Phys. Chem.* **1990**, *94*, 5041.

(12) (a) Mikami, N.; Okabe, A.; Suzuki, I. *J. Phys. Chem.* **1988**, *92*, 1858. (b) Mikami, N.; Suzuki, I.; Okabe, A. *J. Phys. Chem.* **1987**, *91*, 5242.

(13) (a) Lipert, R. J.; Colson, S. D. *J. Phys. Chem.* **1990**, *94*, 2358. (b) Lipert, R. J.; Colson, S. D. *J. Chem. Phys.* **1988**, *89*, 4579. (c) Lipert, R. J.; Bermudez, G.; Colson, S. D. *J. Phys. Chem.* **1988**, *92*, 3801.

(14) (a) Gonohe, N.; Abe, H.; Mikami, N.; Ito, M. *J. Phys. Chem.* **1985**, *89*, 3642. (b) Oikawa, A.; Abe, H.; Mikami, N.; Ito, M. *J. Phys. Chem.* **1983**, *87*, 5083.

methylamine cluster solvation and shifts to lower n as expected for a molecule of large proton affinity (9.8 eV versus 8.8 eV for NH_3).[15] These results are consistent with the recent detection of ground-state ion-pair structures for 3-hydroxyflavone in formamide solution[16] and for 2-naphthol–triethylamine complexes in certain solvent solutions.[17] In addition, Herschbach and coworkers reported formation of ground ion-pair states for the cluster complexes $HX(NH_3)_n$ [X = Cl ($n \geq 1$), Br ($n \geq 1$), and I ($n \geq 3$)].[18]

We derive crude estimates of the equilibrium constant K_a between the locally excited S_1 state and the ion-pair state as a function of n. The acidity of phenol in water at 300 K is reported to be $pK_a = 10$ and $pK_a^* = 4$ for the S_0 and S_1 states, respectively.[19] The threshold for ESPT in $PhOH^*\cdot(NH_3)_n$ occurs between $n = 4$ and 5, from which we estimate values of $\Delta G^* \simeq 0$ and $pK_a^* \simeq 0$ for $n = 4$ or 5. This leads to the value $\Delta G = 0.36$ eV (8.3 kcal/mol). ΔG can also be estimated from the Förster expression[20]

$$\Delta G^* - \Delta G = h\nu_{A^-H^+} - h\nu_{AH} \quad (1a)$$

$$= 2.303kT(pK_a^* - pK_a) \quad (1b)$$

(where we have assumed that $\Delta S \simeq 0$ in eq 1a). The frequencies correspond to the origin transitions of the ion pair and locally excited states, respectively. The former value is difficult to determine because of the broad bandshape for ion-pair transitions. We choose the half-maximum position on the short-wavelength side of the bandshape. For PhOH in monoethylamine clusters, this occurs at 330 nm ($h\nu_{A^-H^+} = 3.76$ eV).[11] For $h\nu_{AH}$ we assume a maximum solvent shift of 0.25 eV from the isolated molecular transition at 4.51 eV.[12] This yields a value of $\Delta G = 0.50 \pm 0.20$ eV for $PhOH\cdot(NH_3)_n$ at $n = 4$–5.

The value of ΔG (and therefore K_a) decreases with increasing n because the sequential addition of NH_3 stabilizes the ion-pair state more than the locally excited state. We express this change by

$$\Delta G_i = \Delta G_{i-1} + D_{i,i-1} - D^{H^+}_{i,i-1} \quad (2)$$

$D_{i,i-1}$ corresponds to the binding energy for $PhOH\cdot B_i \rightarrow PhOH\cdot B_{i-1} + B$. We approximate this value by the NH_3–NH_3 dimer energy of 0.15 eV.[21] $D^{H^+}_{i,i-1}$ describes the binding energy for $PhO^-H^+B_i \rightarrow PhO^-H^+B_{i-1} + B$, which we approximate by the reported stepwise solvation energies for $B\cdot H^+B_i \rightarrow B\cdot H^+B_{i-1} + B$.[22] If the reported value $D^{H^+}_{5,4} = 0.33$ eV (for B = NH_3)[22] is appropriate to our system, then ΔG decreases by 0.18 eV in going from $n = 4$ to $n = 5$. Because the value of K_a is very small for these cluster sizes, it is not known whether we are directly ionizing $n = 4$ and 5 ion pairs or ionizing larger ion-pair clusters that evaporate to stable $n = 4$ and 5 cluster ions.

The ion-pair and ionic clusters are expected to be especially stable for sizes $n = 4$ and 5 due to filling of the solvent or coordination shell about the proton. We consider an ammonium ion core NH_4^+, which has four binding sites. The ion pair $PhO^-H^+(NH_3)_n$ has a shell closing at $n = 4$ due to bonding of PhO^- and three NH_3 molecules about NH_4^+. (The cation cluster corresponding to ionization of PhO^- is also stable.) A fifth NH_3 molecule allows a potentially stable cyclical structure to form by providing a proton donor bond to the oxygen and a proton acceptor bond to a first-shell NH_3 molecule. (A cyclical solvent structure forces the hydrogen bonds to bend in smaller solvent cluster sizes; cf. section 6.) The dissociative ion $H^+(NH_3)_n$ is particularly stable

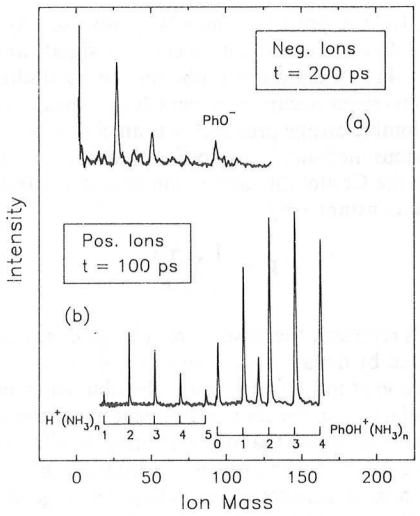

Figure 4. Resonance–ionization mass spectra for negative- and positive-ion detection. Picosecond excitation conditions were $\lambda_1 = 266$ nm and $\lambda_2 = 532$ nm. The negative-ion spectrum in (a) did not change up to $t = 1$ ns. We tentatively assign the PhO^- peak. The other major ion signals (unassigned) occur at ~1, 27, and 52 amu (±2 amu). The negative-ion signals were $<10^{-3}$ the intensity of the positive ion signals in (b). The e^- signal at 0 amu (not plotted) is at least 10^3 greater than the negative-ion signals. The signal at 121 amu in (b) is an unidentified impurity.

at $n = 5$ because of the closed-form structure of four NH_3 molecules about NH_4^+.[22,23] Additional NH_3 molecules add to the second shell where the influence of the proton charge is reduced. These solvent molecules experience less ion–dipole interactions and are, therefore, bound more weakly to the cluster. This is evident by the abrupt decrease in ion intensity of $PhOH^+(NH_3)_n$ and $H^+(NH_3)_n$ for $n > 5$.

4.2. Contact versus Solvent-Separated Ion Pairs. The probability of an ion pair separating under the forces of the solvent depends on the thermal energy kT relative to the Coulombic attraction V_e and on the solvation energy of free ions relative to contact ions.[24–26] To experimentally probe for ion-pair separation, we recorded negative-ion mass spectra using the λ_1–t–λ_2 sequence. $\lambda_1 = 266$ nm was used to initiate ESPT in $PhOH\cdot(NH_3)_n$, and $\lambda_2 = 532$ nm was used to excite the resultant ion-pair excited states $PhOH^*{}^-H^+(NH_3)_n$ in an attempt to dissociate the ion pair. The delay time t was varied up to 1 ns. If the ion pair separates because $V_e \leq kT$, then the cluster should photodissociate efficiently into two oppositely charged ions. We assume the following competition for contact ion pairs (CIPs) versus solvent-separated ion pairs (SSIPs) under λ_2 excitation

$$PhO^*{}^-H^+B_n \xrightarrow[h\nu_2]{} PhOH^+B_n + e \rightarrow PhO + H^+B_n + e \quad \text{(CIP)} \quad (3a)$$

$$PhO^*{}^-B\ H^+B_{n-1} \xrightarrow[h\nu_2]{} PhO^*{}^- + H^+B_n \quad \text{(SSIP)} \quad (3b)$$

where 532-nm excitation is used because it has sufficient energy to dissociate SSIPs ($h\nu_2 = 2.33$ eV $> V_e$). The excess energy ($h\nu_2 - V_e$) is also less than the electron affinity of $PhO^*{}^-$ (≥ 2.4 eV).[27] CIPs are less likely to dissociate and more likely to ionize, yielding only positively charged ions (reaction 3a).

Positive- and negative-ion mass spectra were recorded under nearly identical conditions. The results in Figure 4 provide no evidence of negative-ion formation from SSIP dissociation. The negative-ion signal intensities are more than 3 orders of magnitude

(15) Lias, S. G.; Liebman, J. F.; Levin, R. D. *J. Phys. Chem. Ref. Data* **1984**, *13*, 695.
(16) Parthenopoulos, D. A.; Kasha, M. *Chem. Phys. Lett.* **1990**, *173*, 303.
(17) Bisht, P. B.; Tripathi, H. B.; Pant, D. D. *Chem. Phys.* **1990**, *147*, 173.
(18) Cheung, J. T.; Dixon, D. A.; Herschbach, D. R. *J. Phys. Chem.* **1988**, *92*, 2536.
(19) Ireland, J. F.; Wyatt, P. A. H. *Adv. Phys. Org. Chem.* **1976**, *12*, 131.
(20) (a) Förster, Th. *Z. Electrochem.* **1950**, *54*, 532. (b) Weller, A. *Prog. React. Kinet.* **1961**, *1*, 187.
(21) Ceyer, S. T.; Tiedemann, P. W.; Mahan, B. H.; Lee, Y. T. *J. Chem. Phys.* **1979**, *70*, 14.
(22) (a) Kebarle, P. *Annu. Rev. Phys. Chem.* **1977**, *28*, 445. (b) Grimsrud, E. P.; Kebarle, P. *J. Am. Chem. Soc.* **1973**, *95*, 7939.
(23) (a) Price, J. M.; Crofton, M. W.; Lee, Y. T. *J. Chem. Phys.* **1989**, *91*, 2749. (b) Price, J. M.; Crofton, M. W.; Lee, Y. T. *J. Phys. Chem.* **1991**, *95*, 2182.
(24) Robinson, B. H. In *Proton-Transfer Reactions*; Caldin, C., Gold, V., Eds.; Wiley: New York, 1975; p 121.
(25) Kosower, E. M.; Huppert, D. *Annu. Rev. Phys. Chem.* **1986**, *37*, 127.
(26) Onsager, L. *J. Chem. Phys.* **1934**, *2*, 599.
(27) (a) Moylan, C. R.; Brauman, J. I. *Annu. Rev. Phys. Chem.* **1983**, *34*, 187. (b) Comita, P. B.; Brauman, J. I. *Science* **1985**, *227*, 863.

lower than for the positive ions. We also used λ_2 = 355-nm excitation (3.49 eV) but did not observe any significant difference from Figure 4a. We did not probe for the possibility that CIP → SSIP conversion occurs over very long times (≫1 ns).

The Coulombic escape probability is an old problem developed for a continuous medium,[26] but not for clusters as far as we know. We express the Coulombic attraction in a structureless solvent of dielectric constant ϵ by

$$V = \frac{1}{2\epsilon}\sum_{i,j}\frac{q_i q_j}{r_{ij}} \tag{4}$$

where the q's represent the solvent-free charge densities at specific sites separated by distance r_{ij}. The value of ϵ reflects the extent of delocalization of the ion-pair charge distribution by polarization. Dielectric polarization occurs when solvent molecules orient their dipole moments to oppose that of the ion pair, in effect neutralizing the attractive force. Strong solvent hydrogen bonds can impede this process in small clusters by restricting the range of geometries over which the solvent molecules can reorient.

Calculated Coulombic potential energy curves as a function of cluster size n were reported in paper 1[6] using theoretical charge distributions for PhO^-[28] and $H^+(NH_3)_n$.[29] The potential V as a function of r_{OH} exhibits equilibrium bond lengths r_e ranging from 1.5 Å (n = 0) to 1.9 Å (n = 5) and well depths $|V_e|$ of 5.2 eV (n = 0), 3.1 eV (n = 1), and 2.7 eV (n = 5). These calculations ignore dielectric polarization effects other than that due to the calculated charge distributions in $H^+(NH_3)_n$. From the ratio of $|V_e|(n=0)$ to $|V_e|(n=5)$, one obtains a crude estimate of $\epsilon \simeq 2$ for cluster size n = 5 (eq 4). This value, however, may be underestimated considering the bulk-phase value of ϵ = 25 (77 K).[30,31]

The extent of charge delocalization due to polarization by reorienting solvent molecules is limited in clusters. The stability of the $PhO^*{}^-H^+(NH_3)_5$ cluster is due to the NH_3 solvent shell that surrounds the NH_4^+ core. These first-shell solvent molecules are strongly bound and restricted from efficiently overlapping with the dipolar O–H ion-pair bond. Although there is evidence that the solvent undergoes some structural reorganization in response to proton transfer ion-pair formation,[6] the reduction of V_e is not expected to be substantial.[32] Droz et al. measured shifts in the ion-pair emission bandshape for 2-naphthol·$(NH_3)_n$ cluster excitation.[33] They suggested that solvent-separated ion pairs may be forming for larger cluster sizes ($n \geq 10$). Our results for PhOH·$(NH_3)_n$ indicate that the CIP structure is stable for these cold (~100 K) and small size ($n \leq 15$) clusters, at least over the short measurement time of 1 ns. Charge delocalization undoubtedly occurs; however, NH_4^+ remains strongly bound to PhO^-.

5. Solvated Phenol Dimers

The phenol molecule (like many other aromatic acids and bases, e.g., carboxylic acids and certain amines) forms a stable dimer in solution.[24] The excited-state acidity of aromatic dimer acids has never been measured because of the difficulty in distinguishing the properties of the dimer from the more abundant monomer. This difficulty is circumvented in mass spectrometric studies of clusters. The reaction rate of excited-state (S_1) phenol dimer in $(NH_3)_n$ solvent clusters was measured by detecting the $[PhOH]_2^+(NH_3)_n$ ion signal (Figure 5). Whereas phenol monomer undergoes an abrupt change in reaction rate from n = 4 (>1 ns) to n = 5 (60 ps),[5,6] similar behavior for the dimer acid is not evident. The decay traces in Figure 5 show progressively faster rates with increasing n; however, it cannot be established

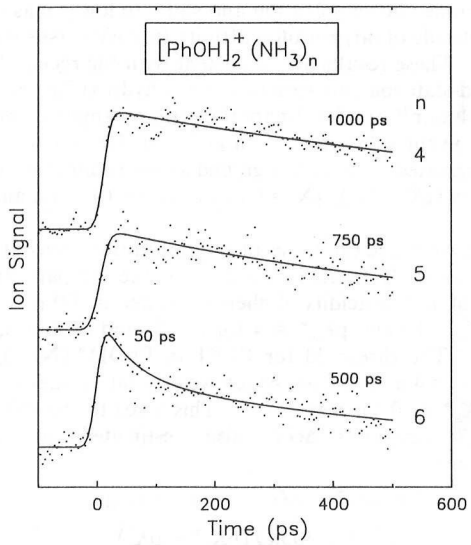

Figure 5. Time dependence for the excited-state dimer cluster $[PhOH]_2{}^*(NH_3)_n$. Single-exponential curves are calculated for n = 4 and 5. The sum of two exponential curves is calculated for n = 6. Decay times are listed above the curves.

that this is due to ESPT. There is some indication of a ~50-ps response for n = 6, followed by a slower decay of about 500 ps, which we discuss below. Finally, we caution that our ability to detect phenol dimer reaction depends on the locally excited and ion-pair states having different probabilities of dissociative ionization. This is clearly the case for solvated phenol monomer (cf. section 3);[5-8] we do not expect the dimer case to be too dissimilar.

The apparent inhibition of proton transfer in phenol dimer relative to phenol monomer in comparable solvent clusters can be explained by the nature of the dimer bond. Spectroscopic evidence[34,35] indicates that the dimer has a linear hydrogen-bond structure with inequivalent phenol molecules. Type I phenol has

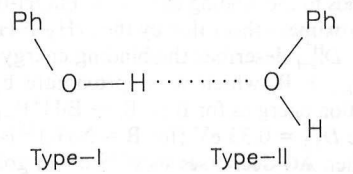

a restricted proton, which should quench ESPT to the solvent. Type II phenol has a free proton available to the solvent. The propensity for ESPT from the dimer depends on (1) the relative absorption cross sections for type I and type II phenol, (2) the excess vibrational energy following S_1 absorption at a given photon energy, and (3) the location and structure of the solvent molecules about the dimer. The $S_0 \rightarrow S_1$ origin transition frequencies for the type I proton-donor structure and the type II proton-acceptor structure are red-shifted (by 303 cm^{-1}) and blue-shifted (by 353 cm^{-1}), respectively, relative to the isolated monomer transition at 275.1 nm.[34,36] The type I and type II phenol transitions are then expected to be red-shifted by NH_3 solvation.

The properties mentioned above provide a basis for interpreting the results in Figure 5. If type II phenol is blue-shifted relative to the monomer, then the lack of ESPT at n = 5 (where monomer reacts)[6] can be attributed to the lower excess energy of photoexcitation. The fast component at n = 6 may then reflect the cluster size threshold for type II ESPT. The slow component is attributed to type I phenol excitation decay (slow ESPT or other processes). It is interesting to speculate about the structure of

(28) Pross, A.; Radom, L.; Taft, R. W. *J. Org. Chem.* **1980**, *45*, 818.
(29) Deakyne, C. A. *J. Phys. Chem.* **1986**, *90*, 6625.
(30) Weast, R. C., Ed. *Handbook of Chemistry and Physics*, 56th ed.; CRC Press: Cleveland, OH, 1975.
(31) Strictly speaking, the dielectric constant ϵ assumes a continuous and structureless medium; hence, we use the term loosely when referring to clusters.
(32) The reduction in the value of V_e occurs by lowering of the asymptotic energy, not by raising of the minima energy.
(33) Droz, T.; Knochenmuss, R.; Leutwyler, S. *J. Chem. Phys.* **1990**, *93*, 4520.
(34) Fuke, K.; Kaya, K. *Chem. Phys. Lett.* **1983**, *94*, 97.
(35) Felker, P. M. Personal communication, to be published.
(36) The hydroxy oxygen loses negative charge density upon $S_0 \rightarrow S_1$. The strength of a hydrogen bond after electronic excitation will, therefore, increase when phenol is the proton donor and decrease when phenol is the proton acceptor. This explains the red-shift (type I) and blue-shift (type II) absorptions in phenol dimer.

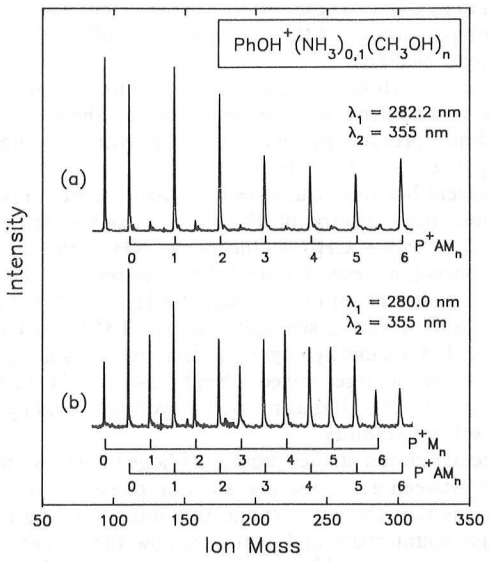

Figure 6. Two-color nanosecond resonance–ionization mass spectra for $PhOH{\cdot}(NH_3)_m(CH_3OH)_n$ recorded for different λ_1 excitation wavelengths. Pulse energies were 50 μJ (282.2 nm), 25 μJ (280.0 nm), and 2 mJ (355 nm) focused to 3-mm-diameter at the molecular beam. P = phenol, A = NH_3, and M = CH_3OH.

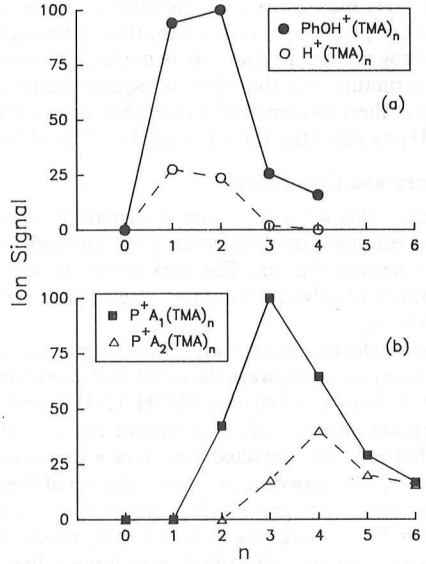

Figure 7. Cluster ion distributions for λ_1–t–λ_2 picosecond resonance–ionization of $PhOH{\cdot}(NH_3)_m(TMA)_n$. λ_1 = 266 nm (10 μJ, 2-mm diameter); t = 100 ps; P = phenol and A = NH_3. (a) λ_2 = 532 nm (1 mJ, 3-mm diameter), (b) λ_2 = 355 nm (0.2 mJ, 3-mm diameter).

the $(NH_3)_n$ solvent cluster about the dimer. One would expect the most favorable bonding site for solvent to be that which surrounds the type II phenol proton, thus facilitating ESPT in a manner similar to the monomer reaction. However, if the type I proton site diverts NH_3 molecules, then an optimum proton-accepting solvent core may fail to form about the free proton, thus inhibiting ESPT.

6. Solvent Structure and Solute–Solvent Bonding Sites

How solvent molecules aggregate about a reactive solute molecule in solution has never been established experimentally. Molecular cluster studies offer the opportunity of providing this information. However, one difficulty is that for cluster sizes that truly reflect closing of solvent shells about a solute molecule, much of the specificity and details of the experiment are lost. Spectroscopic data,[37] which can provide geometry information, are often rendered unresolvable. Hence, it is never quite clear where the solvent molecules reside with regard to the solute reactive sites. In this section we present mass spectra of phenol seeded in *mixed* solvent clusters, which reveal some of the details of the solvent structure and solute–solvent bonding sites.

Information on solute–solvent bonding strengths and solvent structure are obtained from spectral shifts and solvent-size distributions in the mass spectra of clusters. The $S_0 \rightarrow S_1$ origin transition (0,0) of phenol is at 275.1 nm.[38] The spectral shift by sequential addition of solvent molecules is given by

$$\Delta E^{0,0}_{i,i-1} = D_{i,i-1} - D^*_{i,i-1} \qquad (5)$$

where $D_{i,i-1}$ and $D^*_{i,i-1}$ are the binding energies of the ith solvent molecule in the phenol S_0 and S_1 states. D^* is generally greater than D for solute–solvent bonds, in which case eq 5 predicts a red shift. This property holds when phenol is a proton donor.[36] Phenol forms a stronger bond to NH_3 than to CH_3OH as determined from the origin transitions of 280.0 nm ($PhOH{\cdot}NH_3$)[11] and 278.3 nm ($PhOH{\cdot}CH_3OH$).[38] These relative bond strengths are consistent with the relative gas-phase proton affinities of NH_3 (8.8 eV) and CH_3OH (7.9 eV).[15]

Two-color resonance ionization mass spectra were recorded in Figure 6 of phenol solvated in the mixed cluster $PhOH(NH_3)_m(CH_3OH)_n$. For λ_1 = 282 nm, a single series of clusters corresponding to $PhOH^+NH_3(CH_3OH)_n$ is observed (Figure 6a). A pure $PhOH^+(CH_3OH)_n$ series is observed only at shorter wavelength (λ_1 = 280 nm, Figure 6b), indicating that a PhOH–NH_3 bond is responsible for the red shift of the clusters observed in Figure 6a. Although NH_3 forms a more stable bond to PhOH than CH_3OH, the remaining solvent structure is dominated by CH_3OH bonds to NH_3 in the first solvent shell and by self-association in the outer solvent layers. These results have important implications to proton-transfer reactions in solution. In paper 1,[6] we showed that a single CH_3OH molecule in an otherwise pure NH_3 solvent cluster can slow down the rate of reaction by over an order of magnitude. Because CH_3OH does not have as high a proton affinity as NH_3, its *intrusion* into the first solvent shell effectively "poisons" the proton-transfer reaction. Similar behavior was observed in solution by Robinson and co-workers for 1- and 2-naphthol in mixed H_2O and alcohol (CH_3OH and C_2H_3OH) solvents.[39] They ascribed their results to the necessity of forming a pure solvent cluster core to efficiently abstract the proton.

Solvent distributions were obtained for phenol solvated in the mixed solvent cluster $(NH_3)_m(TMA)_n$ (where TMA stands for trimethylamine). This solvent system is interesting because TMA has a much higher proton affinity than NH_3 (9.8 eV versus 8.8 eV)[15] but forms only a limited hydrogen-bond network. The neat TMA solvent ion $PhOH^+(TMA)_n$ in Figure 7a has a peak stability at n = 1–2, reflecting the lack of hydrogen-bonding sites. The proton-transfer product $H^+(TMA)_n$, likewise, peaks at n = 1. Phenol forms a much stronger bond to TMA than to NH_3 (0.56 eV versus 0.29 eV, respectively);[12] however, for larger mixed solvent clusters, it is advantageous for NH_3 to bond to phenol in order to create hydrogen-bonding sites for TMA. The distribution of $PhOH^+NH_3(TMA)_n$ clusters peaks at n = 3 in Figure 7b, suggesting a structure in which NH_3 forms a direct O–H···N bond to phenol, and the first solvent shell is filled by TMA molecules that hydrogen-bond to the three available sites on NH_3. For two NH_3 molecules, $(TMA)_n$ peaks at n = 4 in Figure 7b. Although five hydrogen-bonding sites are presumably available for TMA, steric hindrance from the bulky methyl groups of TMA may present obstacles to full solvent coordination. Alternatively, the

(37) (a) Peteanu, L. A.; Levy, D. H. *J. Phys. Chem.* **1988**, *92*, 6554. (b) Howells, B. D.; Martinez, M. T.; Palmer, T. F.; Simons, J. P.; Walters, A. *J. Chem. Soc., Faraday Trans.* **1990**, *86*, 1949. (c) Connell, L. L.; Corcoran, T. C.; Joireman, P. W.; Felker, P. M. *J. Phys. Chem.* **1990**, *94*, 1229. (d) Champagne, B. B.; Pfanstiel, J. F.; Plusquellic, D. F.; Pratt, D. W.; van Herpen, W. M.; Meerts, W. L. *J. Phys. Chem.* **1990**, *94*, 6.

(38) Oikawa, A.; Abe, H.; Mikami, N.; Ito, M. *J. Phys. Chem.* **1983**, *87*, 5083.

(39) (a) Lee, J.; Griffin, R. D.; Robinson, G. W. *J. Chem. Phys.* **1985**, *82*, 4920. (b) Lee, J.; Robinson, G. W.; Webb, S. P.; Phillips, L. A.; Clark, J. H. *J. Am. Chem. Soc.* **1986**, *108*, 6538. (c) Lee, J.; Robinson, G. W. *J. Chem. Phys.* **1984**, *81*, 1203.

secondary NH_3 may form a six-membered cylical structure by bonding to the phenoxy oxygen atom, thus reducing the number of free hydrogen sites to four. It is unclear, however, whether a cyclical structure is stable since it requires bending hydrogen bonds, nor is there evidence of a blue shift upon addition of the second NH_3 as expected for a proton donor bond to phenoxy.[36]

7. Summary and Conclusions

The goal of this work is to gain information on the solvation of chemical reactions, on a molecular level, through time-resolved studies of molecular clusters. The work presented here underscores the importance of solvent structure. We summarize our results in the following:

1. Ground electronic ion-pair states of phenol, stabilized in $(NH_3)_n$ solvent clusters, were detected that have long-lived absorption at 355 nm and ionize to $PhOH^+(NH_3)_n$ and $H^+(NH_3)_n$. The absorption corresponds to a known ion-pair transition of solvated PhO^-H^+. The detected ions show a strong enhancement at $n = 4$ and 5, corresponding to a stable closing of the first solvent coordination shell. The ground electronic state value of K_a is very small at $n = 5$ but increases with n; hence, much of the signal may originate from ion-pair excitation of large values of n, which then evaporate to stable cluster sizes upon ionization.

2. No evidence of solvent-separated ion pairs was observed. The yield of negative ions (e.g., PhO^-) expected from photodissociation of SSIPs was at least 3 orders of magnitude less than the positive ions formed by the competitive process of dissociative ionization of CIPs. These results are consistent with calculated Coulomb potentials and the low dielectric (bulk) polarization of these small clusters.

3. The formation of phenol dimer inhibits the rate of ESPT to the solvent cluster relative to the monomer. The self-association in the dimer prevents at least one of the hydroxy protons from bonding directly to the solvent.

4. Solvent bonding structures were deduced from resonance–ionization mass spectra of PhOH in mixed solvent clusters $(NH_3)_mB_n$. For B = CH_3OH, the solvent NH_3 forms the stronger bond to phenol; however, CH_3OH then preferentially fills the first coodination shell about the protonated NH_3. For B = TMA, the solute PhOH forms a stronger bond to TMA than to NH_3. However, TMA lacks hydrogen-bonding sites for solvent growth. Consequently, in larger mixed solvent clusters, NH_3 rather than TMA bonds to PhOH, thus providing hydrogen-bonding sites for overall solvent stability.

Molecular cluster studies provide a bridge to understanding the relation between gas-phase and solution-phase chemistry. It is not obvious that there is a connection until one focuses on the gas-phase counterpart and examines how the potential curves change by sequential addition of solvent molecules. The solvation properties in solution then follow clearly from the cluster analogy.

Acknowledgment. This work was supported by the Aerospace Sponsored Research program.

Registry No. PhOH, 108-95-2; NH_3, 7664-41-7; $(CH_3)_3N$, 75-50-3.